Effective-field-theory analysis of the three-dimensional random-field Ising model on isometric lattices

Ümit Akıncı, Yusuf Yüksel,* and Hamza Polat†
Department of Physics, Dokuz Eylül University, TR-35160 Izmir, Turkey
(Received 1 April 2011; published 3 June 2011)

An Ising model with quenched random magnetic fields is examined for single-Gaussian, bimodal, and double-Gaussian random-field distributions by introducing an effective-field approximation that takes into account the correlations between different spins that emerge when expanding the identities. Random-field distribution shape dependencies of the phase diagrams and magnetization curves are investigated for simple cubic, body-centered-cubic, and face-centered-cubic lattices. The conditions for the occurrence of reentrant behavior and tricritical points on the system are also discussed in detail.

DOI: 10.1103/PhysRevE.83.061103 PACS number(s): 75.10.Hk, 75.30.Kz, 75.50.Lk

I. INTRODUCTION

The Ising model [1,2], which was originally introduced as a model describing the phase-transition properties of ferromagnetic materials, has been widely examined in statistical mechanics and condensed matter physics. Over the course of time, basic conclusions of this simple model have been improved by introducing new concepts such as disorder effects on the critical behavior of the systems in question. The Ising model in a quenched random field (RFIM), which has been studied over three decades, is an example of this situation. The model which is actually based on the local fields acting on the lattice sites which are taken to be random according to a given probability distribution was introduced for the first time by Larkin [3] for superconductors and later generalized by Imry and Ma [4]. A lower critical dimension d_c of the RFIM has remained an unsolved mystery for many years and various theoretical methods have been introduced. For example, the domain-wall argument of Imry and Ma [4] suggests that a transition should exist in three and higher dimensions for finite temperature and randomness, which means that $d_c = 2$ [5–8]. On the contrary, dimensional reduction arguments [9] conclude that the system should not have a phase transition at finite temperature in three dimensions (3D) or fewer, so $d_c = 3$ [10–13]. On the other hand, Frontera and Vives [14] showed that a two-dimensional ferromagnetic RFIM with a Gaussian random-field distribution exhibits order at zero temperature.

At the same time, a great many theoretical and experimental works have paid attention to the RFIM and quite noteworthy results have been obtained. For instance, it has been shown that diluted antiferromagnets such as $Fe_xZn_{1-x}F_2$ [15,16], $Rb_2Co_xMg_{1-x}F_4$ [17,18], and $Co_xZn_{1-x}F_2$ [18] in a uniform magnetic field just correspond to a ferromagnet in a random uniaxial magnetic field [19,20]. The following studies have been devoted to investigate the phase diagrams of these systems in depth, and in the mean-field level it was found that different random-field distributions lead to different phase diagrams for infinite dimensional models. For example, using a Gaussian probability distribution, Schneider and Pytte [21] have shown that phase diagrams of the model exhibit only second-order phase-transition properties. Following the same methodology, Andelman [22] discussed the order of the low-temperature transition in terms of the maxima of the distribution function. On the other hand, Aharony [23] and Matthis [24] have introduced bimodal and trimodal distributions, respectively, and they have reported the observation of tricritical behavior. In a recent series of papers, phase-transition properties of infinite dimensional RFIMs with symmetric double- [25] and triple- [26] Gaussian random fields have also been studied by means of a replica method and a rich variety of phase diagrams have been presented. The situation has also been handled on 3D lattices with nearest-neighbor interactions by a variety of theoretical works such as effective-field theory (EFT) [27–31], Monte Carlo (MC) simulations [32–35], pair approximation (PA) [36], and the series expansion (SE) method [37]. By using EFT, Borges and Silva [27] studied the system for square ($q = 4$) and simple cubic (sc) ($q = 6$) lattices, and they observed a tricritical point only for ($q \geqslant 6$). Similarly, Sarmento and Kaneyoshi [29] investigated the phase diagrams of RFIMs by means of EFT with correlations for a bimodal field distribution, and they concluded that reentrant behavior of second order is possible for a system with ($q \geqslant 6$). Recently, Fytas *et al.* [34] applied MC simulations on a sc lattice. They found that the transition remains continuous for a bimodal field distribution, while Hadjiagapiou [38] observed reentrant behavior and confirmed the existence of a tricritical point for an asymmetric bimodal probability distribution within the mean-field approximation based on a Landau expansion.

Conventional EFT approximations include spin-spin correlations resulting from the usage of the Van der Waerden identities, and provide results that are superior to those obtained within the traditional MFT. However, these conventional EFT approximations are not sufficient enough to improve the results, due to the usage of a decoupling approximation (DA) that neglects the correlations between different spins that emerge when expanding the identities. Therefore, taking these correlations into consideration will improve the results of conventional EFT approximations. In order to overcome this point, recently we proposed an approximation that takes into

*Also at Dokuz Eylül University, Graduate School of Natural and Applied Sciences, Turkey.
†hamza.polat@deu.edu.tr

account the correlations between different spins in the cluster of a considered lattice [39–43]. Namely, an advantage of the approximation method proposed by these studies is that no decoupling procedure is used for the higher-order correlation functions. On the other hand, as far as we know, EFT studies in the literature dealing with RFIMs are based only on discrete probability distributions (bimodal or trimodal). Hence, in this paper we intent to study the phase diagrams of the RFIM with single-Gaussian, bimodal, and double-Gaussian random-field distributions on isometric lattices.

The organization of the paper is as follows: In Sec. II we briefly present the formulations. The results and discussions are presented in Sec. III, and finally Sec. IV contains our conclusions.

II. FORMULATION

In this section, we give the formulation of the present study for a sc lattice with $q = 6$. A detailed explanation of the method for bcc and fcc lattices can be found in the Appendix. As a sc lattice, we consider a 3D lattice which has N identical spins arranged. We define a cluster on the lattice which consists of a central spin labeled S_0, and q perimeter spins being the nearest neighbors of the central spin. The cluster consists of $(q + 1)$ spins being independent from the spin operator $\hat{S}$. The nearest-neighbor spins are in an effective field produced by the outer spins, which can be determined by the condition that the thermal average of the central spin is equal to that of its nearest-neighbor spins. The Hamiltonian describing our model is

$$H = -J \sum_{\langle i,j \rangle} S_i^z S_j^z - \sum_i h_i S_i^z, \tag{1}$$

where the first term is a summation over the nearest-neighbor spins with $S_i^z = \pm 1$ and the second term represents the Zeeman interactions on the lattice. Random magnetic fields are distributed according to a given probability distribution function. The present study deals with three kinds of field distribution, namely, a normal distribution which is defined as

$$P(h_i) = \left(\frac{1}{2\pi\sigma^2}\right)^{1/2} \exp\left[-\frac{h_i^2}{2\sigma^2}\right], \tag{2}$$

with a width σ and zero mean, a bimodal discrete distribution

$$P(h_i) = \frac{1}{2}\left[\delta(h_i - h_0) + \delta(h_i + h_0)\right], \tag{3}$$

where half of the lattice sites are subject to a magnetic field h_0 and the remaining lattice sites have a field $-h_0$, and a double-peaked Gaussian distribution

$$P(h_i) = \frac{1}{2}\left(\frac{1}{2\pi\sigma^2}\right)^{1/2} \left\{\exp\left[-\frac{(h_i - h_0)^2}{2\sigma^2}\right] + \exp\left[-\frac{(h_i + h_0)^2}{2\sigma^2}\right]\right\}. \tag{4}$$

In a double-peaked distribution defined in Eq. (4), random fields $\pm h_0$ are distributed with equal probability and the form of the distribution depends on the h_0 and σ parameters, where σ is the width of the distribution.

According to the Callen identity [44] for the spin-1/2 Ising ferromagnetic system, the thermal average of the spin variables at the site i is given by

$$\left\langle \{f_i\} S_i^z \right\rangle = \left\langle \{f_i\} \tanh\left[\beta\left(J \sum_j S_j + h_i\right)\right]\right\rangle, \tag{5}$$

where j expresses the nearest-neighbor sites of the central spin and $\{f_i\}$ can be any function of the Ising variables as long as it is not a function of the site. From Eq. (5) with $f_i = 1$, the thermal and random-configurational averages of a central spin can be represented on a sc lattice by introducing the differential operator technique [45,46]

$$m_0 = \left\langle S_0^z \right\rangle_r = \left\langle\left\langle \prod_{j=1}^{q=6} \left[\cosh(J\nabla) + S_j^z \sinh(J\nabla)\right]\right\rangle\right\rangle_r \times F(x)|_{x=0}, \tag{6}$$

where ∇ is a differential operator, q is the coordination number of the lattice, and the inner $\langle \cdots \rangle$ and the outer $\langle \cdots \rangle_r$ brackets represent the thermal and configurational averages, respectively. The function $F(x)$ in Eq. (6) is defined by

$$F(x) = \int dh_i P(h_i) \tanh[\beta(x + h_i)], \tag{7}$$

and it has been calculated by numerical integration and by using the distribution functions defined in Eqs. (2)–(4). By expanding the right-hand side of Eq. (6) we get the longitudinal spin correlation as

$$\begin{aligned} \langle\langle S_0 \rangle\rangle_r = {} & k_0 + 6k_1 \langle\langle S_1 \rangle\rangle_r + 15k_2 \langle\langle S_1 S_2 \rangle\rangle_r + 20k_3 \langle\langle S_1 S_2 S_3 \rangle\rangle_r \\ & + 15k_4 \langle\langle S_1 S_2 S_3 S_4 \rangle\rangle_r + 6k_5 \langle\langle S_1 S_2 S_3 S_4 S_5 \rangle\rangle_r \\ & + k_6 \langle\langle S_1 S_2 S_3 S_4 S_5 S_6 \rangle\rangle_r. \end{aligned} \tag{8}$$

The coefficients in Eq. (8) are defined as follows:

$$\begin{aligned} k_0 &= \cosh^6(J\nabla) F(x)|_{x=0}, \\ k_1 &= \cosh^5(J\nabla) \sinh(J\nabla) F(x)|_{x=0}, \\ k_2 &= \cosh^4(J\nabla) \sinh^2(J\nabla) F(x)|_{x=0}, \\ k_3 &= \cosh^3(J\nabla) \sinh^3(J\nabla) F(x)|_{x=0}, \\ k_4 &= \cosh^2(J\nabla) \sinh^4(J\nabla) F(x)|_{x=0}, \\ k_5 &= \cosh(J\nabla) \sinh^5(J\nabla) F(x)|_{x=0}, \\ k_6 &= \sinh^6(J\nabla) F(x)|_{x=0}. \end{aligned} \tag{9}$$

Next, the average value of the perimeter spin in the system can be written as follows, and it is found as

$$\begin{aligned} m_1 = \langle\langle S_1 \rangle\rangle_r &= \langle\langle \cosh(J\nabla) + S_0 \sinh(J\nabla) \rangle\rangle_r F(x + \gamma), \\ &= a_1 + a_2 \langle\langle S_0 \rangle\rangle_r. \end{aligned} \tag{10}$$

For the sake of simplicity, the superscript z is omitted from the left- and right-hand sides of Eqs. (8) and (10). The coefficients in Eq. (10) are defined as

$$\begin{aligned} a_1 &= \cosh(J\nabla) F(x + \gamma)|_{x=0}, \\ a_2 &= \sinh(J\nabla) F(x + \gamma)|_{x=0}. \end{aligned} \tag{11}$$

In Eq. (11), $\gamma = (q - 1)A$ is the effective field produced by the $(q - 1)$ spins outside of the system and A is an unknown parameter to be determined self-consistently. Equations (8)

and (10) are the fundamental correlation functions of the system. When the right-hand side of Eq. (6) is expanded, the multispin correlation functions appear. The simplest approximation, and one of the most frequently adopted, is to decouple these correlations according to

$$\left\langle\left\langle S_i S_j \cdots S_l \right\rangle\right\rangle_r \cong \langle\langle S_i \rangle\rangle_r \left\langle\left\langle S_j \right\rangle\right\rangle_r \cdots \langle\langle S_l \rangle\rangle_r , \tag{12}$$

for $i \neq j \neq \cdots \neq l$ [47]. The main difference in the method used in this study from the other approximations in the literature emerges in comparison with any DA when expanding the right-hand side of Eq. (6). In other words, one advantage of the approximation method used in this study is that such a kind of decoupling procedure is not used for the higher-order correlation functions. For a spin-1/2 Ising system in a random field, taking Eqs. (8) and (10) as a basis, we derive a set of linear equations of the spin correlation functions in the system. At this point, we assume that (i) the correlations depend only on the distance between the spins and (ii) the average values of a central spin and its nearest-neighbor spin (it is labeled as the perimeter spin) are equal to each other with the fact that, in the matrix representations of spin operator $\hat{S}$, the spin-1/2 system has the property $(\hat{S})^2 = 1$. Thus, the number of linear equations obtained for a sc lattice ($q = 6$) reduces to 12 and the complete set is as follows:

$$\begin{aligned}
\langle\langle S_1\rangle\rangle_r &= a_1 + a_2\langle\langle S_0\rangle\rangle_r,\\
\langle\langle S_1S_2\rangle\rangle_r &= a_1\langle\langle S_1\rangle\rangle_r + a_2\langle\langle S_0S_1\rangle\rangle_r,\\
\langle\langle S_1S_2S_3\rangle\rangle_r &= a_1\langle\langle S_1S_2\rangle\rangle_r + a_2\langle\langle S_0S_1S_2\rangle\rangle_r,\\
\langle\langle S_1S_2S_3S_4\rangle\rangle_r &= a_1\langle\langle S_1S_2S_3\rangle\rangle_r + a_2\langle\langle S_0S_1S_2S_3\rangle\rangle_r,\\
\langle\langle S_1S_2S_3S_4S_5\rangle\rangle_r &= a_1\langle\langle S_1S_2S_3S_4\rangle\rangle_r + a_2\langle\langle S_0S_1S_2S_3S_4\rangle\rangle_r,\\
\langle\langle S_1S_2S_3S_4S_5S_6\rangle\rangle_r &= a_1\langle\langle S_1S_2S_3S_4S_5\rangle\rangle_r + a_2\langle\langle S_0S_1S_2S_3S_4S_5\rangle\rangle_r,\\
\langle\langle S_0\rangle\rangle_r &= k_0 + 6k_1\langle\langle S_1\rangle\rangle_r + 15k_2\langle\langle S_1S_2\rangle\rangle_r + 20k_3\langle\langle S_1S_2S_3\rangle\rangle_r\\
&\quad +15k_4\langle\langle S_1S_2S_3S_4\rangle\rangle_r\\
&\quad +6k_5\langle\langle S_1S_2S_3S_4S_5\rangle\rangle_r + k_6\langle\langle S_1S_2S_3S_4S_5S_6\rangle\rangle_r,\\
\langle\langle S_0S_1\rangle\rangle_r &= 6k_1 + (k_0 + 15k_2)\langle\langle S_1\rangle\rangle_r + 20k_3\langle\langle S_1S_2\rangle\rangle_r + 15k_4\langle\langle S_1S_2S_3\rangle\rangle_r\\
&\quad +6k_5\langle\langle S_1S_2S_3S_4\rangle\rangle_r + k_6\langle\langle S_1S_2S_3S_4S_5\rangle\rangle_r,\\
\langle\langle S_0S_1S_2\rangle\rangle_r &= (6k_1 + 20k_3)\langle\langle S_1\rangle\rangle_r + (k_0 + 15k_2 + 15k_4)\langle\langle S_1S_2\rangle\rangle_r\\
&\quad +6k_5\langle\langle S_1S_2S_3\rangle\rangle_r + k_6\langle\langle S_1S_2S_3S_4\rangle\rangle_r,\\
\langle\langle S_0S_1S_2S_3\rangle\rangle_r &= (6k_1 + 20k_3 + 6k_5)\langle\langle S_1S_2\rangle\rangle_r + (k_0 + 15k_2 + 15k_4 + k_6)\langle\langle S_1S_2S_3\rangle\rangle_r,\\
\langle\langle S_0S_1S_2S_3S_4\rangle\rangle_r &= (6k_1 + 20k_3 + 6k_5)\langle\langle S_1S_2S_3\rangle\rangle_r + (k_0 + 15k_2 + 15k_4 + k_6)\langle\langle S_1S_2S_3S_4\rangle\rangle_r,\\
\langle\langle S_0S_1S_2S_3S_4S_5\rangle\rangle_r &= (6k_1 + 20k_3 + 6k_5)\langle\langle S_1S_2S_3S_4\rangle\rangle_r\\
&\quad +(k_0 + 15k_2 + 15k_4 + k_6)\langle\langle S_1S_2S_3S_4S_5\rangle\rangle_r.
\end{aligned} \tag{13}$$

If Eq. (13) is written in the form of a 12×12 matrix and solved in terms of the variables x_i [$(i = 1,2,\ldots,12)$ (e.g., $x_1 = \langle\langle S_1\rangle\rangle_r$, $x_2 = \langle\langle S_1S_2\rangle\rangle_r$, $x_3 = \langle\langle S_1S_2S_3\rangle\rangle_r, \ldots$)] of the linear equations, all of the spin correlation functions can be easily determined as functions of the temperature and Hamiltonian and random-field parameters. Since the thermal and configurational average of the central spin is equal to that of its nearest-neighbor spins within the present method, the unknown parameter A can be numerically determined by the relation

$$\langle\langle S_0\rangle\rangle_r = \langle\langle S_1\rangle\rangle_r \quad \text{or} \quad x_7 = x_1. \tag{14}$$

By solving Eq. (14) numerically at a given fixed set of Hamiltonian and random-field parameters we obtain the parameter A. Then we use the numerical values of A to obtain the spin correlation functions which can be found from Eq. (13). Note that $A = 0$ is always the root of Eq. (14) corresponding to the disordered state of the system. The nonzero root of A

TABLE I. Critical temperature k_BT_c/J at $h_0/J = 0$ and $\sigma = 0$ obtained by several methods and the present work for $q = 6,8,12$.

Lattice	EBPA [48]	CEFT [49]	PA [50]	EFT [51]	BA [52]	EFRG [53]	MFRG [54]	MC [55]	SE [56]	Present work
sc	4.8108	4.9326	4.9328	5.0732	4.6097	4.85	4.93	4.51	4.5103	4.5274
bcc		6.9521				6.88	6.95	6.36	6.3508	6.5157
fcc		10.9696							9.7944	10.4986

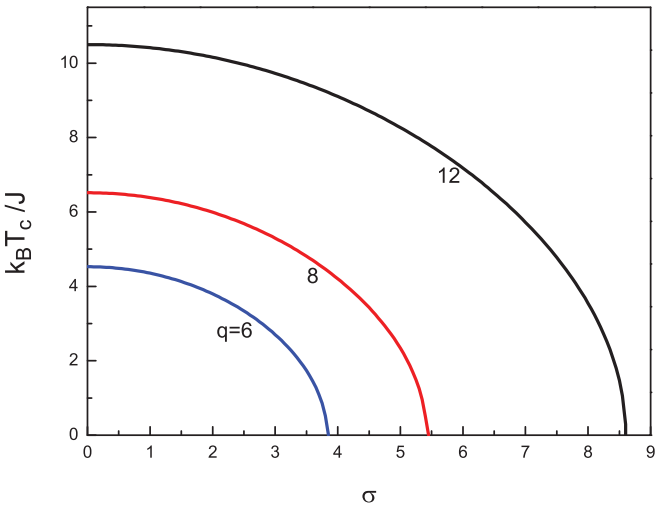

FIG. 1. (Color online) Phase diagrams of sc ($q = 6$), bcc ($q = 8$), and fcc ($q = 12$) lattices in a ($k_BT_c/J - \sigma$) plane corresponding to a single-Gaussian distribution of random fields. The numbers on each curve denote the coordination numbers.

in Eq. (14) corresponds to the long-range-ordered state of the system. Once the spin correlation functions have been evaluated then we can give the numerical results for the thermal and magnetic properties of the system. Since the effective field γ is very small in the vicinity of k_BT_c/J, we can obtain the critical temperature for the fixed set of Hamiltonian and random-field parameters by solving Eq, (14) in the limit of $\gamma \to 0$, and then we can construct the whole phase diagrams of the system. Depending on the Hamiltonian and random-field parameters, there may be two solutions [i.e., two critical temperature values satisfy Eq. (14)] corresponding to the first (or second) and second-order phase-transition points, respectively. We determine the type of the transition by looking at the temperature dependence of magnetization for selected values of system parameters.

III. RESULTS AND DISCUSSION

In this section, we discuss how the type of random-field distribution effects the phase diagrams of the system. Also, in order to clarify the type of transitions in the system, we give the temperature dependence of the order parameter.

A. Phase diagrams of single-Gaussian distribution

The form of single-Gaussian distribution which is defined in Eq. (2) is governed by only one parameter σ, which is the width of the distribution. In Fig. 1, we show the phase diagram of the system for sc, bcc, and fcc lattices in a ($k_BT_c/J - \sigma$) plane. We can clearly see that as σ increases, then the width of the distribution function gets wider and the randomness effect of the magnetic-field distribution on the system becomes significantly important. Therefore, increasing the σ value causes a decline in the critical temperature k_BT_c/J of the system. We note that the critical temperature of the system reaches zero at $\sigma = 3.8501$, 5.450, and 8.601 for sc ($q = 6$), bcc ($q = 8$), and fcc ($q = 12$) lattices, respectively. Besides, we have not observed any reentrant or tricritical behavior for the single-Gaussian distribution, or, in other words, the system undergoes only a second-order phase transition. The k_BT_c/J value in the absence of any randomness, i.e., when

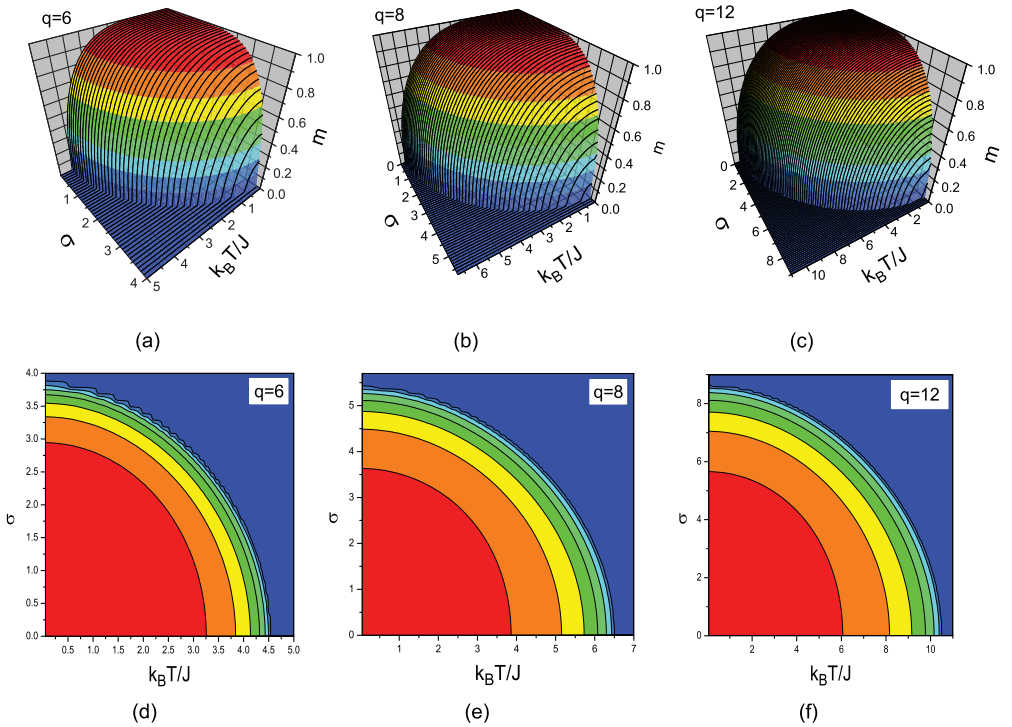

FIG. 2. (Color online) Variation of magnetization with k_BT/J and σ corresponding to the phase diagrams in Fig. 1 for sc, bcc, and fcc lattices. (a)–(c) 3D contour plot surfaces and (d)–(f) projections on a ($k_BT/J - \sigma$) plane.

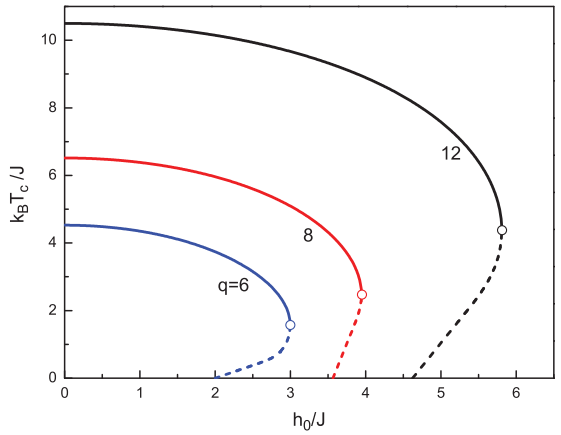

FIG. 3. (Color online) Phase diagrams of the system ($q = 6$, 8, 12) in a ($k_BT_c/J - h_0/J$) plane, corresponding to bimodal random-field distribution. The solid and dashed lines correspond to second- and first-order phase transitions, respectively. The open circles denote the tricritical points.

$\sigma = 0$, is obtained as $k_BT_c/J = 4.5274$, 6.5157, and 10.4986 for $q = 6,8,12$, respectively. These values can be compared with the other works in the literature. Although, to the best of our knowledge, an exact solution for the Ising model does not exist in 3D, it is well known that the SE method agrees well with highly accurate MC simulations, which gives the best approximate values to the known exact results. Therefore, we see in Table I that the present work improves the results of the other works based on EFT. The reason is due to the fact that, in contrast to the previously published works mentioned above, there is no uncontrolled decoupling procedure used for the higher-order correlation functions within the present approximation.

Magnetization surfaces and their projections on the ($k_BT/J - \sigma$) plane corresponding to the phase diagrams shown in Fig. 1 are depicted in Fig. 2 with $q = 6$, 8, and 12. We see that as the temperature increases starting from zero, the magnetization of the system decreases continuously, and it falls rapidly to zero at the critical temperature for all σ values. Moreover, the critical temperature of the system decreases and the saturation value of magnetization curves remains constant for a while then reduces as σ value increases. This is a reasonable result since, if the σ value increases, then the randomness effects increasingly play an important role on the system, and random fields have a tendency to destruct the long-range ferromagnetic order on the system, and hence magnetization weakens. These observations are common properties of all three lattices.

B. Phase diagrams of bimodal distribution

Next, in order to investigate the effect of the bimodal random fields defined in Eq. (3) on the phase diagrams of the system, we show the phase diagrams in a ($k_BT_c/J - h_0/J$) plane and its corresponding magnetization profiles with coordination numbers $q = 6$, 8, and 12 in Figs. 3 and 4. In these figures the solid and dashed lines correspond to second- and first-order phase-transition points, respectively, and the open circles in Fig. 3 denote tricritical points. As seen in Fig. 3, increasing values of h_0/J causes the critical temperature to decrease for a while, then the reentrant behavior of first order occurs at a specific range of h_0/J. According to our calculations, the reentrant phenomena and the first-order phase transitions can be observed within the range of $2.0 < h_0/J < 3.0$ for $q = 6$, $3.565 < h_0/J < 3.95$ for $q = 8$, and $4.622 < h_0/J < 5.81$ for $q = 12$. If the h_0/J value is greater than the upper limits of these field ranges, the system exhibits no phase transition. The tricritical temperatures k_BT_t/J, which are shown as open circles in Fig. 3, are found as $k_BT_t/J = 1.5687$, 2.4751, and 4.3769 for $q = 6$, 8, and 12, respectively.

In Fig. 4, we show two typical magnetization profiles of the system. Namely, the system always undergoes a second-order phase transition for $h_0/J = 1.0$. On the other hand, two successive phase transitions (i.e., a first-order transition is followed by a second-order phase transition) occur at the values of $h_0/J = 2.5$, 3.8, and 5.5 for $q = 6$, 8, and 12, respectively, which puts forward the existence of a first-order reentrant phenomena on the system. We observe that the increasing h_0/J values do not effect the saturation values of magnetization curves.

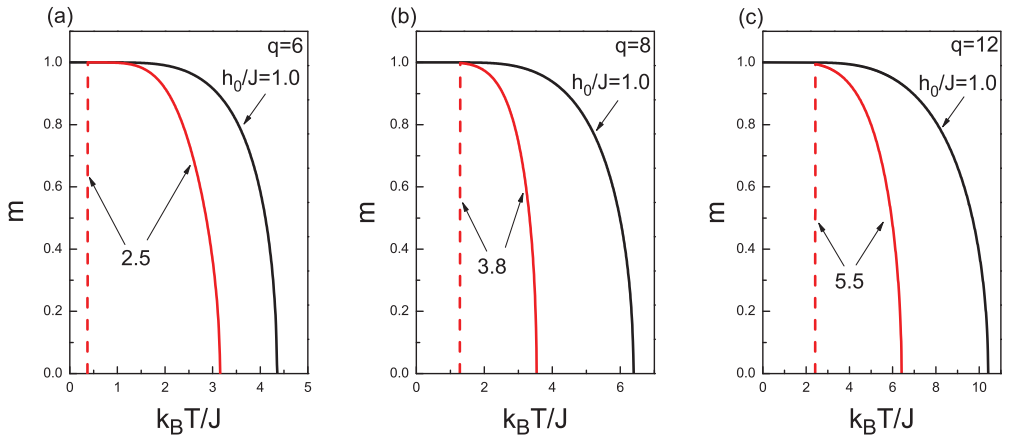

FIG. 4. (Color online) Temperature dependence of magnetization corresponding to Fig. 3 with $\sigma = 0$ and $h_0/J = 1.0,2.5$ for a sc lattice (left-hand panel), $h_0/J = 1.0$ and 3.8 for a bcc lattice (middle panel), and $h_0/J = 1.0$ and 5.5 for a fcc lattice (right-hand panel). The solid and dashed lines correspond to second- and first-order phase transitions, respectively.

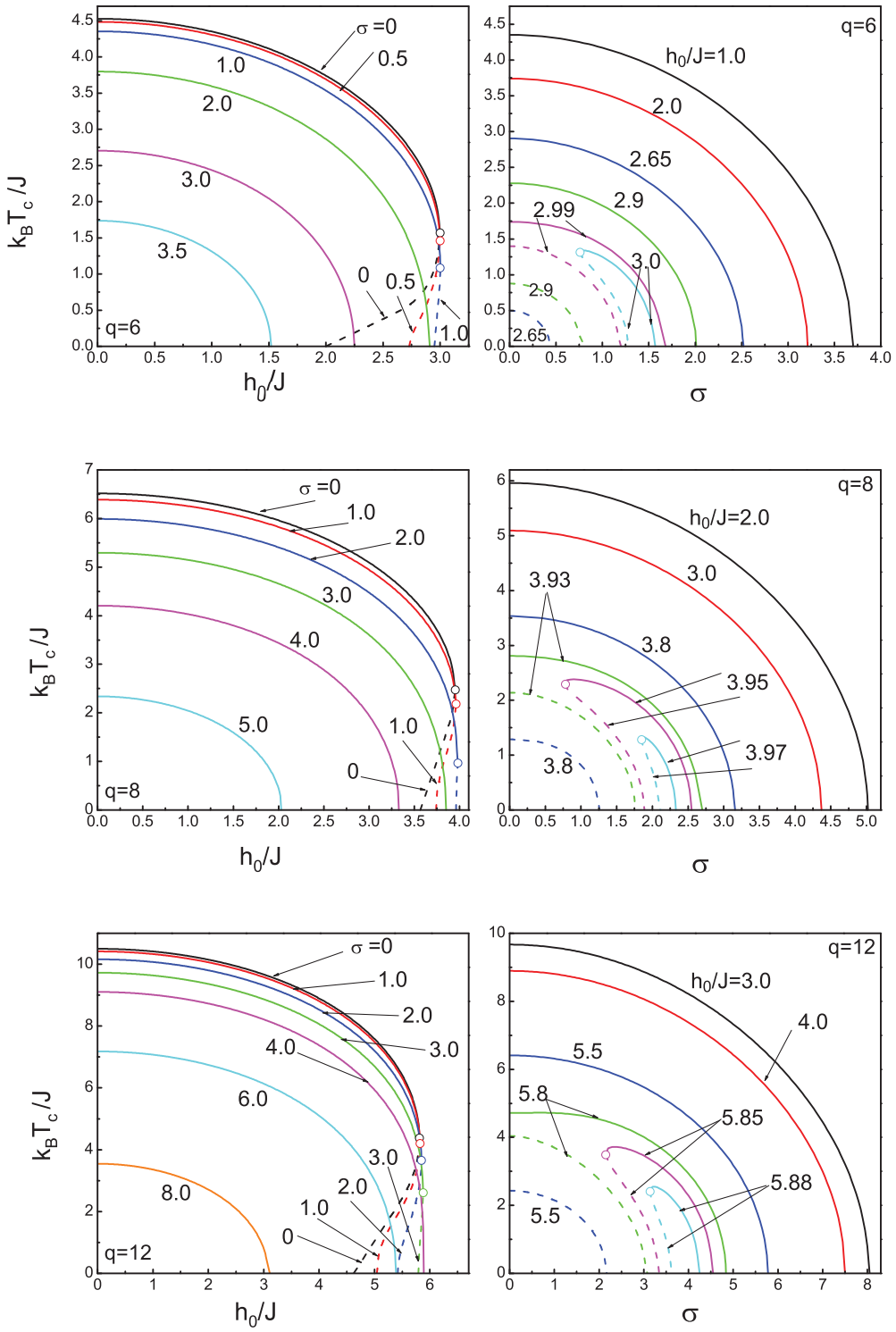

FIG. 5. (Color online) Phase diagrams of the system for a double-Gaussian random-field distribution with $q = 6$, 8, and 12 in $(k_BT_c/J - h_0/J)$ and $(k_BT_c/J - \sigma)$ planes.

C. Phase diagrams of double-Gaussian distribution

To the best of our knowledge, double-Gaussian distribution in Eq. (4) with nearest-neighbor interactions have not yet been examined in the literature. Therefore, it would be interesting to investigate the phase diagrams of the system with random fields corresponding to Eq. (4). Now the shape of the random fields is governed by two parameters h_0/J and σ. As shown in the preceding results, increasing the σ value tends to reduce the saturation value of the order parameter and destructs the second-order phase transitions by decreasing the critical temperature of the system without exposing any reentrant phenomena for $h_0/J = 0$. Besides, as the h_0/J value increases, then the second-order phase-transition temperature decreases

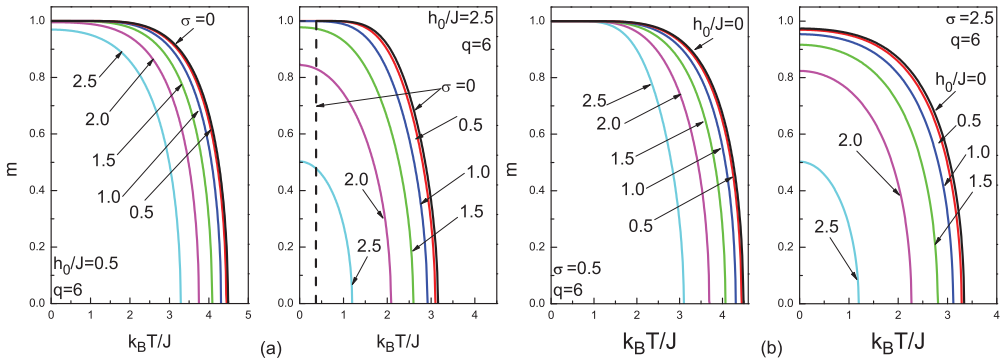

FIG. 6. (Color online) Magnetization curves for a sc lattice corresponding to the phase diagrams in Fig. 5 for a double-Gaussian distribution with some selected values of h_0/J and σ.

again and the system may exhibit a reentrant behavior for $\sigma = 0$, while the saturation value of the magnetization curves remains unchanged. Hence, the presence of both h_0/J and σ on the system should produce a competition effect on the phase diagrams of the system. Figure 5 shows the phase diagrams of the system in $(k_BT_c/J - h_0/J)$ and $(k_BT_c/J - \sigma)$ planes for $q = 6, 8$, and 12. As we can see in the left-hand panels in Fig. 5, the system exhibits tricritical points and reentrant phenomena for a narrow width of the random-field distribution, and as the width σ of the distribution gets wider, then the reentrant phenomena and tricritical behavior disappear. In other words, both the reentrant behavior and tricritical points disappear as the σ parameter becomes significantly dominant on the system. Our results predict that tricritical points depress to zero at $\sigma = 1.421, 2.238$, and 3.985 for $q = 6, 8$, and 12, respectively. For distribution widths greater than these values, all transitions are of second order, and as we further increase the σ value, then the ferromagnetic region gets narrower. Similarly, in the right-hand panels in Fig. 5, we investigate the phase diagrams of the system in a $(k_BT_c/J - \sigma)$ plane with selected values of h_0/J. We note that for the values of $h_0/J \leqslant 2.0$ $(q = 6)$, $h_0/J \leqslant 3.565$ $(q = 8)$, and $h_0/J \leqslant 4.622$ $(q = 12)$, the system always undergoes a second-order phase transition between the paramagnetic and ferromagnetic phases at a critical temperature which decreases with increasing values of h_0/J as in Fig. 1, where $h_0/J = 0$. Moreover, for values of h_0/J greater than these threshold values, the system exhibits a reentrant behavior of first order and the transition lines exhibit a bulge which gets smaller with increasing values of h_0/J, which again means that the ferromagnetic phase region gets narrower. Besides, for $h_0/J > 2.9952$ $(q = 6)$, $h_0/J > 3.9441$ $(q = 8)$, and $h_0/J > 5.8085$ $(q = 12)$, tricritical points appear on the system. In Fig. 6, we show magnetization curves corresponding to the phase diagrams shown in Fig. 5 for a sc lattice. Figure 6(a) shows the temperature dependence of magnetization curves for $q = 6$ with $h_0/J = 0.5$ (left-hand panel) and $h_0/J = 2.5$ (right-hand panel) with selected values of σ. As we can see in Fig. 6(a), as σ increases, then the critical temperature of the system decreases and first-order phase transitions disappear [see the right-hand panel in Fig. 6(a)]. Moreover, the rate of decrease of the saturation value of the magnetization curves increases as h_0/J increases. On the other hand, in Fig. 6(b), the magnetization versus temperature curves have been plotted with $\sigma = 0.5$ (left-hand panel) and $\sigma = 2.5$ (right-hand panel) with some selected values of h_0/J. In this figure, it is clear that saturation values of magnetization curves remain unchanged for $\sigma = 0.5$ and tend to decrease rapidly to zero with increasing values of h_0/J when $\sigma = 2.5$. In addition, as h_0/J increases when the value of σ is fixed, then the critical temperature of the system decreases and the ferromagnetic

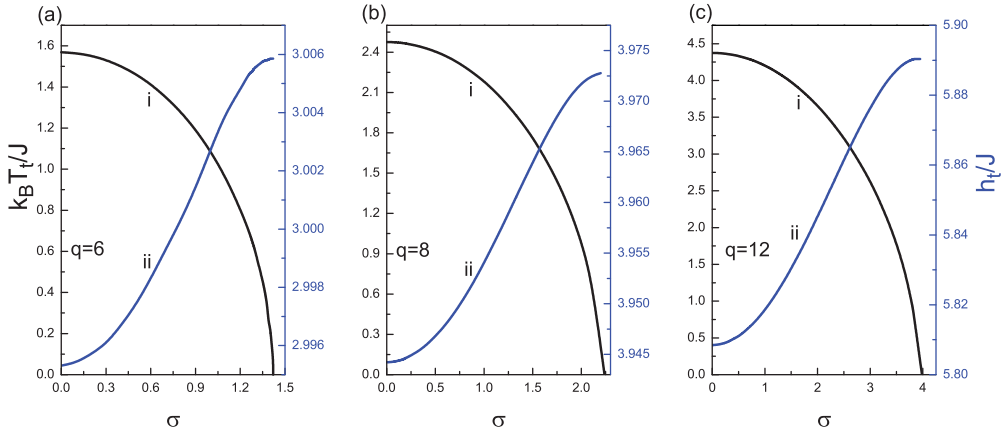

FIG. 7. (Color online) Variations of tricritical temperature k_BT_t/J (i) and tricritical field h_t/J (ii) as function of distribution width (σ) for (a) sc, (b) bcc, and (c) fcc lattices.

phase region of the system gets narrower. These observations show that there is a competition effect originating from the presence of both h_0/J and σ parameters on the phase diagrams and magnetization curves of the system.

Finally, Fig. 7 represents the variation of the tricritical point $(k_BT_t/J, h_t/J)$ with σ for $q = 6$, 8, and 12. As seen from Fig. 7, the k_BT_t/J value decreases monotonically as σ increases and reaches zero at a critical value σ_t. According to our calculations, the critical distribution width σ_t value can be given as $\sigma_t = 1.421$, 2.238, and 3.985 for $q = 6$, 8, and 12, respectively. This implies that the σ_t value depends on the coordination number of the lattice. Besides, h_t/J curves exhibit a relatively small increment with an increasing σ value.

IV. CONCLUSIONS

In this work, we have studied the phase diagrams of a spin-1/2 Ising model in a random magnetic field on sc, bcc, and fcc lattices. We have introduced an effective-field approximation that takes into account the correlations between different spins in the cluster of a considered lattice and examined the phase diagrams as well as magnetization curves of the system for different types of random-field distributions, namely, single-Gaussian, bimodal, and double-Gaussian distributions. For a single-Gaussian distribution, we have found that the system always undergoes a second-order phase transition between the paramagnetic and ferromagnetic phases. For bimodal and double-Gaussian distributions, we have given the proper phase diagrams, especially the first-order transition lines that include reentrant phase-transition regions. Our numerical analysis clearly indicates that such field distributions lead to a tricritical behavior. Moreover, we have discussed a competition effect which arises from the presence of both h_0/J and σ parameters, and we have observed that saturation values of the magnetization curves are strongly related to these effects.

In addition, in the absence of any randomness (i.e., $h_0/J = 0$, $\sigma = 0$) our critical temperature values corresponding to the coordination numbers $q = 6$, 8, and 12 are the best approximate values to the results of MC and SE methods, among the other works given in Table I. As a result, we can conclude that all of the points mentioned above show that our method improves the conventional EFT methods based on decoupling approximation. Therefore, we hope that the results obtained in this work may be beneficial from both theoretical and experimental points of view.

APPENDIX: COMPLETE SET OF CORRELATION FUNCTIONS FOR BCC AND FCC LATTICES

The number of distinct correlations for the spin-1/2 system with q nearest neighbors is $2q - 1$. With the magnetization of the central spin $\langle\langle S_0\rangle\rangle_r$ and its nearest-neighbor spin $\langle\langle S_1\rangle\rangle_r$, there has to be $2q + 1$ unknowns which forms a system of linear equations. The q's of the correlations, which include the central spin, are derived from the central spin magnetization $\langle\langle S_0\rangle\rangle_r$, and rest of the $q - 1$ correlations which include only a perimeter spin are derived from the perimeter spin magnetization expression $\langle\langle S_1\rangle\rangle_r$. Let us label these correlations with x_i, $i = 1,2,\ldots,2q + 1$, such that the first q includes only perimeter spins and the last $q + 1$ includes a central spin. We can represent all of the spin correlations and central and perimeter spin magnetization with x_i as $x_1 = \langle\langle S_1\rangle\rangle_r, x_2 = \langle\langle S_1S_2\rangle\rangle_r, \ldots, x_q = \langle\langle S_1S_2\cdots S_q\rangle\rangle_r, x_{q+1} = \langle\langle S_0\rangle\rangle_r$, $x_{q+2} = \langle\langle S_0S_1\rangle\rangle_r, \ldots$, and $x_{2q+1} = \langle\langle S_0S_1\cdots S_q\rangle\rangle_r$. The complete set of correlation functions for $q = 8$ and 12 can be obtained as the same procedure given between Eqs. (6)–(13) in Sec. II.

The first q ($q = 8$ and 12) correlation functions can be written in a general form as

$$x_1 = a_1 + a_2x_{q+1}, \quad x_i = a_1x_{i-1} + a_2x_{i+q} \quad (i = 2,\ldots,q),$$

where the coefficients are given by

$$a_1 = \cosh(J\nabla)F(x+\gamma)|_{x=0}, \quad a_2 = \sinh(J\nabla)F(x+\gamma)|_{x=0},$$

with $\gamma = (q-1)A$. Similarly, the last $q/2 + 1$ correlation functions are

$$x_i = l_q^{(1)}x_{i-q-2} + l_q^{(2)}x_{i-q-1} \quad (i = 3q/2 + 1,\ldots,2q + 1),$$

where

$$\begin{aligned}
l_8^{(1)} &= 56k_3 + 56k_5 + 8k_7 + 8k_1,\\
l_8^{(2)} &= 70k_4 + k_8 + 28k_2 + k_0 + 28k_6,\\
l_{12}^{(1)} &= 12k_1 + 220k_3 + 220k_9 + 792k_5 + 12k_{11} + 792k_7,\\
l_{12}^{(2)} &= k_0 + 66k_2 + k_{12} + 495k_4 + 495k_8 + 66k_{10} + 924k_6.
\end{aligned}$$

The remaining $q/2$ correlation functions for a bcc lattice ($q = 8$),

$$\begin{aligned}
x_9 &= k_0 + 8k_1x_1 + 28k_2x_2 + 56k_3x_3 + 70k_4x_4 + 56k_5x_5\\
&\quad + 28k_6x_6 + 8k_7x_7 + k_8x_8,\\
x_{10} &= 8k_1 + (28k_2 + k_0)x_1 + 56k_3x_2 + 70k_4x_3 + 56k_5x_4\\
&\quad + 28k_6x_5 + 8k_7x_6 + k_8x_7,\\
x_{11} &= (56k_3 + 8k_1)x_1 + (70k_4 + 28k_2 + k_0)x_2 + 56k_5x_3\\
&\quad + 28k_6x_4 + 8k_7x_5 + k_8x_6,\\
x_{12} &= (56k_3 + 56k_5 + 8k_1)x_2 + (70k_4 + 28k_2 + k_0 + 28k_6)x_3\\
&\quad + 8k_7x_4 + k_8x_5,
\end{aligned}$$

and $q/2$ correlation functions for a fcc lattice ($q = 12$) are given as follows:

$$\begin{aligned}
x_{13} &= k_0 + 12k_1x_1 + 66k_2x_2 + 220k_3x_3 + 495k_4x_4 + 792k_5x_5 + 924k_6x_6\\
&\quad + 792k_7x_7 + 495k_8x_8 + 220k_9x_9 + 66k_{10}x_{10} + 12k_{11}x_{11} + k_{12}x_{12},\\
x_{14} &= 12k_1 + (k_0 + 66k_2)x_1 + 220k_3x_2 + 495k_4x_3 + 792k_5x_4 + 924k_6x_5,\\
&\quad + 792k_7x_6 + 495k_8x_7 + 220k_9x_8 + 66k_{10}x_9 + 12k_{11}x_{10} + k_{12}x_{11},\\
x_{15} &= (12k_1 + 220k_3)x_1 + (k_0 + 66k_2 + 495k_4)x_2 + 792k_5x_3 + 924k_6x_4,
\end{aligned}$$

$$
\begin{aligned}
&+792k_7x_5 + 495k_8x_6 + 220k_9x_7 + 66k_{10}x_8 + 12k_{11}x_9 + k_{12}x_{10},\\
x_{16} &= (12k_1 + 220k_3 + 792k_5)x_2 + (k_0 + 66k_2 + 495k_4 + 924k_6)x_3,\\
&+792k_7x_4 + 495k_8x_5 + 220k_9x_6 + 66k_{10}x_7 + 12k_{11}x_8 + k_{12}x_9,\\
x_{17} &= (12k_1 + 220k_3 + 792k_5 + 792k_7)x_3 + (k_0 + 66k_2 + 495k_4 + 495k_8 + 924k_6)x_4,\\
&+220k_9x_5 + 66k_{10}x_6 + 12k_{11}x_7 + k_{12}x_8,\\
x_{18} &= (12k_1 + 220k_3 + 220k_9 + 792k_5 + 792k_7)x_4\\
&+(k_0 + 66k_2 + 495k_4 + 495k_8 + 66k_{10} + 924k_6)x_5 + 12k_{11}x_6 + k_{12}x_7,
\end{aligned}
$$

with

$$k_i = \cosh^{q-i}(J\nabla)\sinh^i(J\nabla)F(x)|_{x=0}, \quad i = 0,\ldots,q,$$

where q is the coordination number. Since the first $2q$ equations are independent of the correlation labeled x_{2q+1}, it is not necessary to include this correlation function in the set of linear equations. Therefore it is adequate to take $2q$ linear equations for calculations.

ACKNOWLEDGMENTS

One of the authors (Y.Y.) would like to thank the Scientific and Technological Research Council of Turkey (TÜBİTAK) for partial financial support. This work has been completed at the Dokuz Eylül University, Graduate School of Natural and Applied Sciences. Partial financial support from SRF (Scientific Research Fund) of Dokuz Eylül University (2009.KB.FEN.077) is also acknowledged.

[1] E. Ising, Z. Phys. **31**, 253 (1925).
[2] L. Onsager, Phys. Rev. **65**, 117 (1944).
[3] A. I. Larkin, Sov. Phys. JETP **31**, 784 (1970).
[4] Y. Imry and S. K. Ma, Phys. Rev. Lett. **35**, 1399 (1975).
[5] G. Grinstein and S. K. Ma, Phys. Rev. Lett. **49**, 685 (1982).
[6] J. F. Fernandez, G. Grinstein, Y. Imry, and S. Kirkpatrick, Phys. Rev. Lett. **51**, 203 (1983).
[7] J. Z. Imbrie, Phys. Rev. Lett. **53**, 1747 (1984).
[8] J. Bricmont and A. Kupiainen, Phys. Rev. Lett. **59**, 1829 (1987).
[9] G. Parisi and N. Sourlas, Phys. Rev. Lett. **43**, 744 (1979).
[10] K. Binder, Y. Imry, and E. Pytte, Phys. Rev. B **24**, 6736 (1981).
[11] E. Pytte, Y. Imry, and D. Mukamel, Phys. Rev. Lett. **46**, 1173 (1981).
[12] D. Mukamel and E. Pytte, Phys. Rev. B **25**, 4779 (1982).
[13] A. Niemi, Phys. Rev. Lett. **49**, 1808 (1982).
[14] C. Frontera and E. Vives, Phys. Rev. E **59**, R1295 (1999).
[15] D. P. Belanger, A. R. King, and V. Jaccarino, Phys. Rev. B **31**, 4538 (1985).
[16] A. R. King, V. Jaccarino, D. P. Belanger, and S. M. Rezende, Phys. Rev. B **32**, 503 (1985).
[17] I. B. Ferreira, A. R. King, V. Jaccarino, J. L. Cardy, and H. J. Guggenheim, Phys. Rev. B **28**, 5192 (1983).
[18] H. Yoshizawa, R. A. Cowley, G. Shirane, R. J. Birgeneau, H. J. Guggenheim, and H. Ikeda, Phys. Rev. Lett. **48**, 438 (1982).
[19] S. Fishman and A. Aharony, J. Phys. C **12**, L729 (1979).
[20] J. L. Cardy, Phys. Rev. B **29**, 505 (1984).
[21] T. Schneider and E. Pytte, Phys. Rev. B **15**, 1519 (1977).
[22] D. Andelman, Phys. Rev. B **27**, 3079 (1983).
[23] A. Aharony, Phys. Rev. B **18**, 3318 (1978).
[24] D. C. Mattis, Phys. Rev. Lett. **55**, 3009 (1985).
[25] N. Crokidakis and F. D. Nobre, J. Phys. Condens. Matter **20**, 145211 (2008).
[26] O. R. Salmon, N. Crokidakis, and F. D. Nobre, J. Phys. Condens. Matter **21**, 056005 (2009).
[27] H. E. Borges and P. R. Silva, Physica A **144**, 561 (1987).
[28] Y. Q. Liang, G. Z. Wei, Q. Zhang, Z. H. Xin, and G. L. Song, J. Magn. Magn. Mater. **284**, 47 (2004).
[29] E. F. Sarmento and T. Kaneyoshi, Phys. Rev. B **39**, 9555 (1989).
[30] R. M. Sebastianes and W. Figueiredo, Phys. Rev. B **46**, 969 (1992).
[31] T. Kaneyoshi, Physica A **139**, 455 (1985).
[32] D. P. Landau, H. H. Lee, and W. Kao, J. Appl. Phys. **49**, 1356 (1978).
[33] J. Machta, M. E. J. Newman, and L. B. Chayes, Phys. Rev. E **62**, 8782 (2000).
[34] N. G. Fytas, A. Malakis, and K. Eftaxias, J. Stat. Mech. Theory Exp. (2008), 03015.
[35] N. G. Fytas and A. Malakis, Eur. Phys. J. B **61**, 111 (2008).
[36] E. Albayrak and O. Canko, J. Magn. Magn. Mater. **270**, 333 (2004).
[37] M. Gofman, J. Adler, A. Aharony, A. B. Harris, and M. Schwartz, Phys. Rev. B **53**, 6362 (1996).
[38] I. A. Hadjiagapiou, Physica A **389**, 3945 (2010).
[39] H. Polat, Ü. Akıncı, and İ. Sökmen, Phys. Status Solidi B **240**, 189 (2003).
[40] Y. Canpolat, A. Torgürsül, and H. Polat, Phys. Scr. **76**, 597 (2007).
[41] Y. Yüksel, Ü. Akıncı, and H. Polat, Phys. Scr. **79**, 045009 (2009).
[42] Y. Yüksel and H. Polat, J. Magn. Magn. Mater. **322**, 3907 (2010).
[43] Ü. Akıncı, Y. Yüksel, and H. Polat, Physica A **390**, 541 (2011).
[44] H. B. Callen, Phys. Lett. **4**, I61 (1963).
[45] R. Honmura and T. Kaneyoshi, J. Phys. C **12**, 3979 (1979).
[46] T. Kaneyoshi, Acta Phys. Pol. A **83**, 703 (1993).
[47] I. Tamura and T. Kaneyoshi, Prog. Theor. Phys. **66**, 1892 (1981).
[48] A. Du, H. J. Liu, and Y. Q. Yü, Phys. Status Solidi B **241**, 175 (2004).
[49] T. Kaneyoshi, I. P. Fittipaldi, R. Honmura, and T. Manabe, Phys. Rev. B **24**, 481 (1981).
[50] T. Balcerzak, Physica A **317**, 213 (2003).
[51] T. Kaneyoshi, Rev. Solid State Sci. **2**, 39 (1988).

[52] R. Kikuchi, Phys. Rev. **81**, 988 (1951).
[53] J. R. de Sousa and I. G. Araújo, J. Magn. Magn. Mater. **202**, 231 (1999); M. A. Neto and J. R. de Sousa, Phys. Rev. B **70**, 224436 (2004).
[54] E. E. Reinerhr and W. Figueiredo, Phys. Lett. A **244**, 165 (1998).
[55] D. P. Landau, Phys. Rev. B **16**, 4164 (1977); **14**, 255 (1976); A. M. Ferrenberg and D. P. Landau, *ibid*. **44**, 5081 (1991).
[56] M. E. Fisher, Rep. Prog. Phys. **30**, 615 (1967).